Chemical Geology 269 (2010) 376–385

Contents lists available at ScienceDirect

Chemical Geology

journal homepage: www.elsevier.com/locate/chemgeo

Variations of Sr–Nd–Hf isotopic systematics in basalt during intensive weathering

Jinlong Ma [a,c], Gangjian Wei [a,b,*], Yigang Xu [a], Wenguo Long [a,d]

[a] Key Laboratory of Isotope Geochronology and Geochemistry, Guangzhou Institute of Geochemistry, Chinese Academy of Sciences, Guangzhou 510640, China
[b] Key Laboratory of Marginal Sea Geology, Chinese Academy of Sciences, Guangzhou 510640, China
[c] Graduate School of the Chinese Academy of Sciences, Beijing 100049, China
[d] Hainan Bureau of Geology and Mineral Resources, Haikou 570226, China

ARTICLE INFO

Article history:
Received 26 February 2009
Received in revised form 13 October 2009
Accepted 25 October 2009

Editor: B. Bourdon

Keywords:
Saprolites
Sr–Nd–Hf isotope
Intensive weathering
South China

ABSTRACT

The Sr–Nd–Hf isotopic compositions of both saprolites and parent rocks of a profile of intensively weathered Neogene basalt in Hainan, South China are reported in this paper to investigate changes of isotopic systematics with high masses. The results indicate that all these isotopic systematics show significant changes in saprolites compared to those in corresponding parent rocks. The $^{87}Sr/^{86}Sr$ system was more seriously affected by weathering processes than other isotope systems, with ε_{Sr} drifts 30 to 70 away from those of the parent rocks. In the upper profile (>2.2 m), the Sr isotopes of the saprolites show an upward increasing trend with ε_{Sr} changing from ~50 at 2.2 m to ~70 at 0.5 m, accompanying a upward increasing of Sr concentrations, from ~10 μg/g to ~25 μg/g. As nearly all the Sr of the parent rock has been removed during intensive weathering in this profile, the upward increasing of Sr concentrations in the upper profile suggests import of extraneous Sr. Rainwater in this region, which enriches in Sr (up to 139 μg/L) from seawater, may be the important extraneous source. Thus, the Sr isotopes of the saprolites in the upper profile may be mainly influenced by import of extraneous materials, and the Sr isotopic characteristics may not be retained. In contrast, the ε_{Nd} and ε_{Hf} of the saprolites drift only 0–2.6 and 0–3.7 away from the parent rocks, respectively. The negative drifts of the ε_{Nd} and ε_{Hf} are coupled with Nd and Hf losses in the saprolites; i.e., larger proportions of Nd and Hf loss correspond to lower ε_{Nd} and ε_{Hf}. Compared with the relative high Nd and Hf concentrations of the saprolites, the contributions of extraneous Nd and Hf both from wet and dry deposits of aeolian input are negligible. Thus, the ε_{Nd} and ε_{Hf} changes in the profile are mainly resulted from consecutive removal of the Nd and Hf. Calculation indicates that the $^{143}Nd/^{144}Nd$ and $^{176}Hf/^{177}Hf$ ratios in saprolites are all significantly lower than their initial values in the parent rock. Simply removing part of the Nd and Hf by incongruent decomposing some of the minerals may not account for this. Fractionation should be happen, which ^{143}Nd and ^{176}Hf may be preferentially removed from the profile relative to ^{144}Nd and ^{177}Hf during intensive chemical weathering, resulting in lower $^{143}Nd/^{144}Nd$ and $^{176}Hf/^{177}Hf$ ratios in saprolites relative to the parent rock, even though details for this process is not known. A positive correlation is observed between the ε_{Nd} and ε_{Hf} of the saprolites. Interestingly, the saprolites with a net loss of Nd and Hf in the upper profile show good positive correlation, and the regression line parallels the terrestrial array. By contrast, saprolites with a net gain of Nd and Hf in the lower profile generally show higher ε_{Hf} values at a given ε_{Nd} value, and the regression line between these ε_{Nd} and ε_{Hf} appears to parallel the seawater array. This supports the hypothesis that the contribution of continental Hf from chemical weathering release is the key to the obliquity of the seawater array away from the terrestrial array of the global ε_{Nd} and ε_{Hf} correlation. Our results also indicate that caution is needed when using ε_{Sr}, ε_{Nd}, and ε_{Hf} to trace provenances for sediments and soils.

1. Introduction

Chemical weathering is one of the most important processes that change the chemical composition of the Earth's surface. Quite a number of studies have been carried out in the past several decades to investigate the mobilization and re-distribution of major and trace elements during chemical weathering processes. Thus, the behaviors of most of these elements, under conditions ranging from incipient to extreme weathering, have been well described (Nesbitt, 1979; Nesbitt et al., 1980; Duddy, 1980; Chesworth et al., 1981; Nahon et al., 1982; Middelburg et al., 1988; Banfield and Eggleton, 1989; Price et al., 1991; Marsh, 1991; Nesbitt and Wilson, 1992; Mongelli, 1993; Braun et al., 1993, 1998; Boulange and Colin, 1994; Condie et al., 1995; Walter et al., 1995; Koppi et al., 1996; Nesbitt and Markovics, 1997; Hill et al., 2000; Aubert et al., 2001; Patino et al., 2003; Ma et al., 2007a). Compared to elements, the variations of isotopic systematics

* Corresponding author. Key Laboratory of Marginal Sea Geology, Chinese Academy of Sciences, Guangzhou 510640, China. Tel.: +86 20 85290093; fax: 86 20 85290130.
E-mail address: gjwei@gig.ac.cn (G. Wei).

0009-2541/$ – see front matter © 2009 Elsevier B.V. All rights reserved.
doi:10.1016/j.chemgeo.2009.10.012

during chemical weathering are of relatively less concern. As for the isotopic systematics with high masses, isotopic fractionation during surface processes is generally not considered, in that a definite internal isotopic ratio is adopted to calibrate isotopic fractionation during mass spectrometry measurements. For example, $^{86}Sr/^{88}Sr$, $^{146}Nd/^{144}Nd$, and $^{179}Hf/^{177}Hf$ are generally used for Sr, Nd, and Hf isotope measurements, respectively. However, recent studies indicate that fractionation of Sr isotopic systematics appears to be significant during chemical weathering (De Souza et al., 2007). Significant isotopic fractionation can also be seen in some other isotopic systems during chemical weathering (Wimpenny et al., 2007; Yamaguchi et al., 2007; Stirling et al., 2007; Wiederhold et al., 2007). These observations challenge our general knowledge and indicate the necessity for a more detailed understanding of changes to isotopic systematics during chemical weathering processes.

Among all the isotopic systematics with high masses, Sr and Nd isotopes are the most popular traditional systematics, whereas studies on Hf isotopic systematics have been rapidly expanded in the past decade (Faure and Mensing, 2005). These isotopic systems have been broadly utilized for investigations in many fields of the earth sciences. In addition, the behaviors of Sr, Nd, and Hf are significantly different during chemical weathering. Sr is one of the most active elements during chemical weathering, and is very easily removed from the weathering profile (Nesbitt et al., 1980). Nd is a moderate active element. It can be easily motivated from primary minerals, and tends to be incorporated into secondary minerals during incipient-to-moderate weathering. Yet it is readily removed during intensive weathering (Nesbitt and Wilson, 1992; Nesbitt and Markovics, 1997). Hf is generally believed to be conservative during chemical weathering (Nesbitt and Wilson, 1992; Nesbitt and Markovics, 1997). However, significant Hf mobilization can also be seen during extreme chemical weathering (Ma et al., 2007a). Therefore, studies on these isotopic systematics with different chemical activities may provide a general view on the overall aspects of isotopic variations in response to chemical weathering.

Significant changes in weathering profiles of $^{87}Sr/^{86}Sr$ have been reported in previous studies. These have mainly been attributed to either incongruent decomposing of minerals during incipient-to-moderate weathering because of the heterogeneous $^{87}Sr/^{86}Sr$ ratios in different minerals (Blum and Erel, 1995; Negrel, 2006), or to input of extraneous Sr with different $^{87}Sr/^{86}Sr$ ratios into saprolites that have undergone extensive weathering from aeolian deposits or groundwater (Price et al., 1991; Stewart et al., 2001; Kurtz et al., 2001; Dia et al., 2006). Chemical weathering may slightly alter the Sm/Nd ratio in saprolites, compared to the parent rock (Nesbitt and Markovics, 1997). As a result, the $^{143}Nd/^{144}Nd$ ratios of saprolites could be different from those in parent rocks after a fairly long period of evolution (Ohlander et al., 2000). However, Nd isotope records in weathering profiles, concerning the direct modification of Nd isotopic systematics by chemical weathering, are scarce.

Currently available records generally show very narrow variation ranges for $^{143}Nd/^{144}Nd$ ratios in saprolites, except for those receiving significant extraneous Nd inputs from aeolian deposits (Kurtz et al., 2001; Dia et al., 2006). This appears to indicate that chemical weathering may not significantly alter Nd isotopic systematics. However, studies concerning Nd isotope changes during chemical weathering processes, in particular during intensive chemical weathering, are rare. Details of changes to Nd isotopic systematics are not well described yet. As Nd isotopes are broadly used in tracing provenances for sediments and soils, which are mostly composed of weathering products, knowledge of Nd isotopic variations during chemical weathering is very important to assure the applicability of Nd isotopes as provenance proxies for sediments and soils.

One of the striking results in Hf isotope studies in the past decades is that there exists a broad positive correlation between $^{143}Nd/^{144}Nd$ and $^{176}Hf/^{177}Hf$ in the earth's systems. There are two kinds of global Hf–Nd isotopic correlations. One is called the "terrestrial array", which is well-represented by most of the crustal and mantle rocks (Vervoort et al., 1999). The other is called the "seawater array", which is observed in seawater and authigenic materials deposited from seawater, such as ferromanganese crusts and nodules (Albarede et al., 1998). The $^{176}Hf/^{177}Hf$ ratio in the seawater array is generally higher than that in the terrestrial array for a given $^{143}Nd/^{144}Nd$ ratio (Albarede et al., 1998). The obliquity of the seawater array away from the terrestrial array is generally attributed to inputs of continental Hf. These are due to incongruent release of Hf during chemical weathering on continents, even though the other sources, such as hydrothermal contributions, cannot be ignored (Van De Flierdt et al., 2002, 2004, 2007). Therefore, direct evidence showing the changes in Hf isotopic systematics during chemical weathering are of critical importance for this hypothesis.

We herein report the Sr–Nd–Hf isotopic compositions of both saprolites and parent rocks in a weathering profile developed on Neogene basalt in northern Hainan Island, South China, aiming to highlight the alteration of high-mass isotopic systematics by chemical weathering. This is helpful for better evaluating the applicability of these isotopic systems to geochemical studies on surface processes, and will help to understand the geochemical cycles of these elements on the earth's surface.

2. Materials and analytical methods

The samples that were studied were collected from a laterite profile developed from Neogene basalts in the northern region of Hainan Island, South China. Details of the profile have been described in Ma et al. (2007a). Both saprolites and parent rock were included in this study. The saprolite samples were composed of extremely weathered laterite, and the parent rock is fresh tholeiitic basalt. Details of the sample material, including its mineralogical composition, and its major and trace elements, have also been reported in Ma et al. (2007a).

The sample powders were first baked at 700 °C to destroy organic materials, preceding Sr–Nd–Hf isotopic analysis. For Sr–Nd isotopic analysis, samples were digested using an $HNO_3 + HF$ mixture, and finally dissolved in a 2 N HCl solution. The sample solution was first loaded on a column filled with AG50-X8 cation resin. Both Sr and REEs were trapped on the column. 2 N HCl eluant was used to rinse the column. Sr and REEs were de-trapped from the column using 2 N and 3 N HCl, respectively. The de-trapped REEs were further concentrated using an RE Spec column, and consequently, an LN Spec (HDEHP-based) column was used to separate Nd from REEs. For details of the column chemistry, refer to Wei et al. (2004).

Sr isotopes were measured on a GV Isoprobe-T thermal ionization mass spectrometer (TIMS) at the Institute of Geology and Geophysics, Chinese Academy of Sciences (IGG-CAS). $^{88}Sr/^{86}Sr = 0.1194$ was adopted to calibrate mass bias during measurements, and the NBS SRM 987 standard was repeatedly measured to monitor the quality of the measurements, yielding an average $^{87}Sr/^{86}Sr$ of 0.710250 ± 10 (2σ) ($N = 5$). Nd isotopic measurements were carried out on a MicroMass Isoprobe multi-collector inductively coupled plasma mass spectrometer (MC-ICP-MS) at the Guangzhou Institute of Geochemistry, Chinese Academy of Sciences (GIG-CAS) (for details, refer to Liang et al., 2003). Fractionation of the measured $^{143}Nd/^{144}Nd$ was normalized using $^{146}Nd/^{144}Nd = 0.7219$. A standard Nd solution, JNdi-1, was repeatedly measured together with the samples, and yielded a mean value of 0.512123 ± 0.000008 (2σ) ($N = 10$) for $^{143}Nd/^{144}Nd$.

The samples for Hf isotope analysis were digested using alkali fusion method. For each sample, 0.5 g powder was mixed with 1.0 g $Li_2B_4O_7$ and fused at 1200 °C to make a glass disc. The glass discs were then crushed into small pieces. Fragments of approximately 0.3 g were weighed, and then digested by 2 N HCl. Hf was separated using

an HDEHP column. Hf isotope measurements were taken on a Finnigan Neptune MC-ICP-MS at the IGG-CAS. Hf isotopic fractionation during measurement was calibrated using $^{179}Hf/^{177}Hf = 0.7325$. The quality of the Hf isotopic ratios was monitored by repeatedly measuring Hf isotope standard JMC-475 along with the samples, and the measured $^{176}Hf/^{177}Hf$ for JMC 475 was 0.282162 ± 10 (2σ) ($N = 5$). For details of the analysis method, refer to Li et al. (2005). The Sr–Nd–Hf isotopic ratios, together with their ε_{Sr}, ε_{Nd}, and ε_{Hf} values normalized by chondrite, are listed in Table 1. The Rb, Sr, Sm, Nd, Lu, and Hf concentrations of these samples, which have been reported by Ma et al. (2007a), are also included in Table 1 for comparison.

A USGS basalt rock standard BHVO-2 was measured with the samples, and the results for BHVO-2 were $^{87}Sr/^{86}Sr = 0.703420 \pm 12$ (2σ) ($N = 4$), $^{143}Nd/^{144}Nd = 0.512950 \pm 8$ (2σ) ($N = 4$), and $^{176}Hf/^{177}Hf = 0.283094 \pm 7$ (2σ) ($N = 4$).

Some precipitation samples during winter and summer were collected in Sanya, a coastal city in the southern Hainan Island to monitor the concentration of Sr, Nd and Hf of the rainwater in the coastal regions of Hainan Island. Na and K concentrations and Sr, Nd and Hf concentrations of the precipitation samples were measured using a Dionex ICS 900 ion chromatography (IC) and a PE Elan 6000 inductively coupled plasma mass spectrometry (ICP-MS) at the GIG-CAS. Precision of the concentrations is better than 5%, and the results are listed in Table 2.

3. Results

The variations of ε_{Sr}, ε_{Nd} and ε_{Hf} along the profile are shown in Fig. 1. The corresponding values of the parent rocks are also shown for comparison. The Sr isotope exhibited the largest variation range, with ε_{Sr} varying from about +40 at the bottom of the profile to about +70 at the top. In the lower profile, except for the samples of HK06-12 and HK06-17, the ε_{Sr} of the saprolites exhibit relatively limited variations, from +39.1 to +54.6, while in the upper profile an upward increasing trend is clearly shown with ε_{Sr} changing from +47.2 of HK06-4 at 1.6 m to +69.1 of HK06-1 at 0.5 m. All the ε_{Sr} of the saprolites are markedly higher than that of the parent rock, which was about $+0.33 \pm 0.13$. The Nd isotopes in the lower profile (below 3.5 m) show large variations, with ε_{Nd} changing from +2.75 to +0.32, and in the middle profile (3.2–2.2 m), the variation of ε_{Nd} is relative limited, from +1.0 to +1.2. In the upper profile, the ε_{Nd} shows significant upward decreasing trends, from +1.32 of HK06-5 at 1.9 m to +0.50 of KH06-1 at 0.5 m. Except for the sample of HK06-19 at the bottom profile, all the saprolites show significantly lower ε_{Nd} than that of the parent rock, $+2.90 \pm 0.13$. Similarly, the ε_{Hf} in the lower profile show limited variation range, from +8 to +9, except for the sample of HK06-10 in the middle of the profile (3.2 m), which shows the maximum ε_{Hf} value, $+9.63 \pm 0.36$, close to that of the parent rock, $+9.53 \pm 0.16$. In the upper profile, an upward decreasing trend is clearly shown, with ε_{Hf} changing from +7.43 at 2.20 m to +5.82 at 0.5 m.

The Na, K and Sr concentrations in the precipitation samples range from 1.46 mg/L to 13.9 mg/L, from 0.23 mg/L to 10.0 mg/L and 15.5 μg/L to 139 μg/L, respectively, while the Nd and Hf in the precipitation samples are under the detecting limit of the ICP-MS.

Table 2
Na, Sr, Nd and Hf concentrations of precipitation samples in Sanya.

Sample date	2008/07/07	2008/07/16	2008/12/30	2009/05/22
Na (mg/L)	13.9	7.86	1.46	2.40
K (mg/L)	10.0	1.81	0.23	0.38
Sr (μg/L)	139	19.1	15.5	25.6
Nd (μg/L)	<0.01	<0.01	<0.01	<0.01
Hf (μg/L)	<0.01	<0.01	<0.01	<0.01

4. Discussion

4.1. Sr–Nd–Hf isotope variations during chemical weathering

As Fig. 1 shows, the Sr–Nd–Hf isotopes of the saprolites are significantly different from those in the parent rock. The largest gaps of ε_{Sr}, ε_{Nd}, and ε_{Hf} values between the weathered samples and the parent rock are observed at the top of the profile, where the most extreme weathering occurs. Extreme chemical weathering can motivate most of the elements in parent rock, which results in different parent/daughter ratios for some of the isotopic systems in the saprolites. The trace element records of this profile show dramatic variations in trace element ratios; e.g., the Rb/Sr, Sm/Nd, and Lu/Hf ratios of the parent rock are 0.0586, 0.261, and 0.0455, respectively, whereas these in the topmost sample are 0.375, 0.180 and 0.0135, respectively (Ma et al., 2007a). The significantly higher Rb/Sr and lower Sm/Nd and Lu/Hf ratios in the saprolites appear to correspond

Table 1
Sr–Nd–Hf isotopic compositions of the saprolites and parent rock.

Sample ID	Depth (m)	Rb[a]	Sr[a]	Sm[a]	Nd[a]	Lu[a]	Hf[a]	Th[a]	$^{87}Sr/^{86}Sr$[b]	ε_{Sr}[b]	$^{143}Nd/^{144}Nd$[b]	ε_{Nd}[c]	$^{176}Hf/^{177}Hf$[b]	ε_{Hf}[c]
HK06-1	0.50	9.57	25.5	4.95	27.5	0.20	14.7	9.20	0.709370 ± 7	69.1 ± 0.1	0.512664 ± 10	0.50 ± 0.20	0.282934 ± 10	5.82 ± 0.34
HK06-2	0.90	7.82	25.4	4.85	26.7	0.19	14.2	9.19	0.708702 ± 6	59.6 ± 0.1	0.512657 ± 8	0.38 ± 0.16	0.282932 ± 3	5.76 ± 0.10
HK06-3	1.30	5.32	21.5	4.51	25.2	0.17	13.6	8.58	0.708136 ± 8	51.6 ± 0.1	0.512676 ± 9	0.74 ± 0.18	0.282946 ± 3	6.26 ± 0.09
HK06-4	1.60	4.25	19.0	4.11	22.0	0.15	13.5	7.90	0.707822 ± 7	47.2 ± 0.1	0.512679 ± 7	0.81 ± 0.14	0.282965 ± 3	6.92 ± 0.11
HK06-5	1.90	3.79	13.4	3.62	17.7	0.15	14.7	7.83	0.708081 ± 6	50.8 ± 0.1	0.512705 ± 10	1.32 ± 0.20	0.282970 ± 4	7.10 ± 0.13
HK06-6	2.20	3.89	10.4	4.41	20.2	0.18	14.3	7.10	0.708081 ± 8	50.8 ± 0.1	0.512697 ± 10	1.14 ± 0.20	0.282979 ± 3	7.43 ± 0.12
HK06-7	2.50	3.06	7.71	5.50	23.9	0.23	12.0	5.86	0.708050 ± 6	50.4 ± 0.1	0.512700 ± 9	1.21 ± 0.18	0.283016 ± 7	8.74 ± 0.26
HK06-8	2.80	1.88	3.96	8.29	33.5	0.33	10.9	5.02	0.708225 ± 6	52.9 ± 0.1	0.512691 ± 8	1.04 ± 0.16	0.282996 ± 3	8.04 ± 0.10
HK06-9	3.00	1.76	4.25	8.57	34.1	0.35	7.98	3.72	0.707904 ± 7	48.3 ± 0.1	0.512690 ± 6	1.01 ± 0.12	0.282999 ± 5	8.12 ± 0.16
HK06-10	3.20	2.27	2.39	12.6	51.1	0.49	14.4	5.99	0.707774 ± 7	46.5 ± 0.1	0.512689 ± 8	1.00 ± 0.16	0.283041 ± 10	9.63 ± 0.36
HK06-12	3.50	4.33	3.20	41.0	170	1.54	10.8	4.90	0.706859 ± 8	33.5 ± 0.1	0.512731 ± 8	1.81 ± 0.16	0.283022 ± 3	8.93 ± 0.10
HK06-13	3.65	3.20	1.84	9.87	44.1	0.35	8.78	3.87	0.708234 ± 8	53.0 ± 0.1	0.512669 ± 8	0.60 ± 0.16	0.282997 ± 3	8.05 ± 0.09
HK06-15	3.95	4.45	1.43	16.1	71.6	0.52	11.0	4.74	0.708350 ± 8	54.6 ± 0.1	0.512705 ± 9	1.30 ± 0.18	0.283007 ± 2	8.40 ± 0.07
HK06-16	4.10	5.97	1.36	14.6	62.2	0.48	15.5	6.37	0.708295 ± 7	53.9 ± 0.1	0.512720 ± 9	1.61 ± 0.18	0.283018 ± 5	8.80 ± 0.16
HK06-17	4.20	5.28	2.57	26.9	121	0.83	14.9	5.97	0.706694 ± 6	31.1 ± 0.1	0.512699 ± 9	1.19 ± 0.18	0.283001 ± 3	8.22 ± 0.12
HK06-18	4.30	5.84	2.99	31.2	137	0.99	16.7	6.81	0.707765 ± 5	46.3 ± 0.1	0.512655 ± 9	0.32 ± 0.16	0.283005 ± 4	8.35 ± 0.13
HK06-19	4.40	2.89	5.22	32.5	147	1.09	15.7	6.70	0.707397 ± 9	41.1 ± 0.1	0.512779 ± 10	2.75 ± 0.20	0.282996 ± 2	8.02 ± 0.08
HK06-20	4.50	1.65	2.43	26.0	111	0.92	16.4	6.58	0.707252 ± 9	39.1 ± 0.1	0.512737 ± 9	1.94 ± 0.18	0.283004 ± 4	8.32 ± 0.13
HK06-R1		16.8	286	4.56	17.5	0.24	5.36	2.46	0.704523 ± 9	0.33 ± 0.13	0.512787 ± 8	2.90 ± 0.16	0.283039 ± 4	9.53 ± 0.13

[a] The Rb, Sr, Sm, Nd, Lu, Hf and Th concentrations are from Ma et al. (2007a,b).
[b] Errors for the $^{87}Sr/^{86}Sr$, $^{143}Nd/^{144}Nd$ and $^{176}Hf/^{177}Hf$ are 2σ.
[c] ε values are calculated relative to the chondrite: $\varepsilon = (R_{sample}/R_{chondrite} - 1) \times 10{,}000$, and the isotope ratios for the chondrite are: $^{87}Sr/^{86}Sr = 0.7045$, $^{143}Nd/^{144}Nd = 0.512638$, and $^{176}Hf/^{177}Hf = 0.282769$ (Nowell et al., 1998).

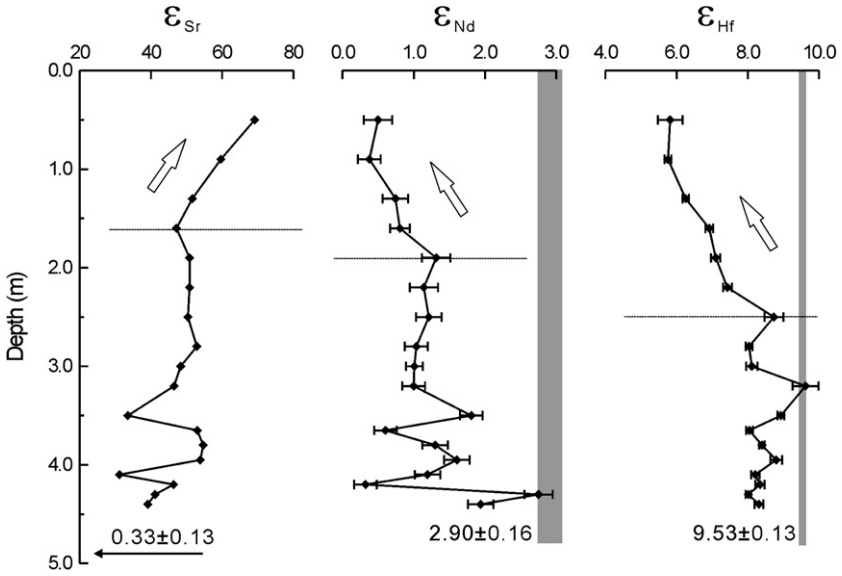

Fig. 1. In-depth variations of the chondrite-normalized ε_{Sr}, ε_{Nd}, and ε_{Hf} of the saprolites. The shaded bars mark the ranges of the chondrite-normalized ε_{Sr}, ε_{Nd}, and ε_{Hf} of the parent rock, and the data are their values with 2σ errors. Note that the ε_{Sr} of the parent rock is too small to show in the diagram.

to the higher $^{87}Sr/^{86}Sr$ and lower $^{143}Nd/^{144}Nd$ and $^{176}Hf/^{177}Hf$ ratios in the saprolites, compared to those in the parent rock. However, the eruption age of the basalt, on which the saprolites developed, is only about 4.0 Ma (Zhu and Wang, 1989). Considering that the decay constants for ^{87}Rb, ^{147}Sm, and ^{176}Lu are very small, at the level of 10^{-11}, the accumulation of radiogenically decayed ^{87}Sr, ^{143}Nd, and ^{176}Hf are negligible. Thus, the Sr–Nd–Hf isotope changes in the saprolites should be caused by direct interference of the Sr–Nd–Hf systematics during chemical weathering.

There are two basic ways to make the isotopes in saprolites different from the parent rock. One is to incorporate extraneous Sr–Nd–Hf with different isotopic composition into a saprolite, and the second is to preferentially remove some isotopes during weathering. The behaviors of these three elements during chemical weathering are significantly different. Sr is one of the most active elements, and is easily removed from the profile during chemical weathering. Nd is easily motivated, but tends to incorporate into weathering products during incipient-to-moderate weathering. In contrast, Hf is generally believed to be conservative during chemical weathering (Nesbitt et al., 1980; Nesbitt and Wilson, 1992). The different behaviors of these elements may account for the difference in the variations of these isotopic systems during chemical weathering.

4.1.1. Variations of Sr and Sr isotopic systematics

Generally, the isotopic composition of fresh basalt is an average of all kinds of minerals and glass masses. Different minerals may have different Rb/Sr ratios and Sr concentrations, and hence different $^{87}Sr/^{86}Sr$ ratios. Preferentially decomposing special minerals (e.g. feldspar) during incipient weathering will result in quickly decreasing of the Sr concentrations and changing of $^{87}Sr/^{86}Sr$ ratios in residual weathering products (Blum and Erel, 1995). Consequently, during extreme weathering processes, nearly all the origin minerals are altered, and the residual Sr contents in weathering products are very low. In our studied profile, nearly all the Sr has been removed. The Sr concentration in the parent rock is 286 μg/g, while the Sr concentrations in the saprolites vary from 1.3 μg/g to 25.6 μg/g. The loss of Sr of the saprolites can be estimated by the percentage changes of Sr/Th ratios relative to the parent rock, assuming that Th is conservative during extreme weathering as:

$$\%change\ of\ ratios = 100 \times [(R_i - R_p)/R_p]$$

where R_i and R_p represent the ratio of element/Th in weathered samples and fresh basalt, respectively (Nesbitt, 1979). The calculated percentage changes of Sr/Th ratios, as well as other elements discussed as follows are listed in Table 3. As shown in Fig. 2, the percentage changes of Sr/Th ratios vary from −97.6 to −99.8, indicating that about 98–100% Sr in the parent rock has been removed from the profile without deducting the possible contribution from extraneous Sr. Accompanying such prominent loss of Sr, the Sr isotopes significantly drift away from that of the parent rock, with the maximum ε_{Sr} drift being up to 69.1. Such a high percentage of Sr loss and large ε_{Sr} drift suggest that the original Sr isotopic composition of the parent rock may not be preserved in saprolites that have undergone extreme weathering.

It is worth noting that the Sr concentrations in the saprolites increase upwards from the middle profile (2.5 m) to upper profile. The intensity of chemical weathering in the top section of this profile is much stronger than that in the lower section. This can be inferred from the major and trace element records, even though the whole

Table 3
Percentage changes of element/Th ratios of the saprolites relative the parent rock and the abundance of kaolinite (unit: %).

Sample ID	Depth (m)	Sr/Th	Nd/Th	Hf/Th	K/Th	Cs/Th	Kaolinite[a] abundance
HK06-1	0.50	−97.6	−58.0	−26.7	−93.5	27.0	82
HK06-2	0.90	−97.6	−59.2	−29.1	−94.3	12.3	73.1
HK06-3	1.30	−97.8	−58.7	−27.3	−95.9	−13.2	79.3
HK06-4	1.60	−97.9	−60.9	−21.6	−96.4	−26.5	73.9
HK06-5	1.90	−98.5	−68.2	−13.8	−97.3	−33.7	43.8
HK06-6	2.20	−98.7	−60.0	−7.6	−97.5	−33.6	64
HK06-7	2.50	−98.9	−42.7	−6.0	−95.8	−35.9	
HK06-8	2.80	−99.3	−6.2	−0.3	−98.6	−44.2	62
HK06-9	3.00	−99.0	28.9	−1.5	−98.1	−35.7	28.3
HK06-10	3.20	−99.7	19.9	10.3	−98.8	−64.6	
HK06-12	3.50	−99.4	387	1.2	−97.1	−38.6	
HK06-13	3.65	−99.6	60.2	4.1	−96.4	−47.0	
HK06-15	3.95	−99.7	112	6.5	−97.0	−45.2	
HK06-16	4.10	−99.8	37.3	11.7	−97.2	−52.8	
HK06-17	4.20	−99.6	185	14.5	−97.1	−47.3	
HK06-18	4.30	−99.6	182	12.5	−97.4	−45.8	
HK06-19	4.40	−99.3	207.8	7.5	−98.4	−57.2	
HK06-20	4.50	−99.7	136.9	14.4	−99.5	−70.9	20

All the element concentrations and kaolinite abundance are from Ma et al. (2007a,b).
[a] Blank indicates that no kaolinite was detected.

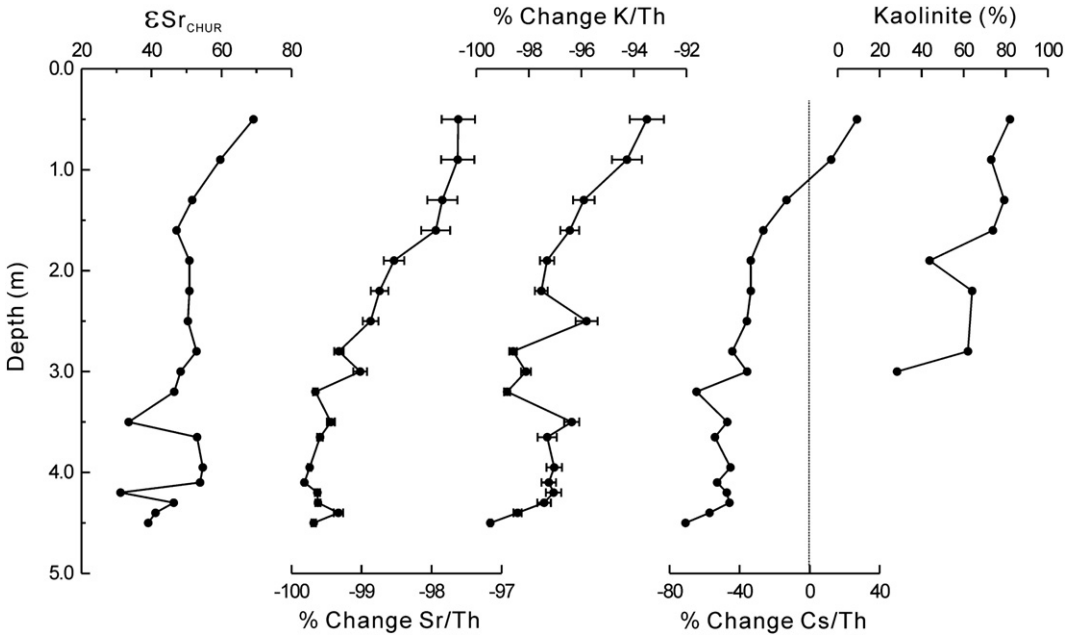

Fig. 2. In-depth variation of the chondrite-normalized ε_{Sr}, the percentage changes of Sr/Th, K/Th, and Cs/Th ratios relative to the parent rock and the kaolinite abundance of the saprolites. The error bars on the percentage of Sr/Th, K/Th and Cs/Th mark their error ranges calculated using Gaussian error transport equation.

profile has been intensively weathered (Ma et al., 2007a). Because Sr is very easily removed, if the Sr in the saprolites is among the residual components after weathering, the Sr concentrations in the top section should be lower than those in the lower section. The upward increase in the Sr concentrations in this profile does not agree with this explanation. Thus, the Sr in these saprolites may mainly be imported from extraneous sources, rather than being residue of the parent rock.

Some alkali and alkali earth elements, such as K, Cs, and Sr, tend to be fixed in the clay minerals by ion exchange or absorption (Nesbitt et al., 1980). The variation patterns of these elements are similar in this profile. Table 3 lists the percentage changes of these elements to Th ratios relative to the parent rock, and they are also shown in Fig. 2. The percentage changes of K/Th, Cs/Th, and Sr/Th ratios all exhibit similar upward increasing trends. The percentage changes of Cs/Th ratios of the top most two samples are even positive, 20 and 12, respectively, indicating import of extraneous materials for these elements. More importantly, this trend is co-incident with an increasing abundance of kaolinite shown in Fig. 2. Considering that the behaviors of all these elements are very active, they are not likely to be retained in saprolites during intensive weathering. The similar variation patterns of these elements and the kaolinite abundance suggest that the K, Sr, and Cs in the upper section of this profile are imported from extraneous sources and their presence are mainly associated with the presence of clay minerals such as kaolinite.

Consequently, the large variation of Sr isotopes of the saprolites may also respond to the import of extraneous Sr. The Sr isotopes of the saprolites also show grossly upward trends in Fig. 2, with ε_{Sr} of about +30 to +40 at the bottom and about +70 at the top section. Fig. 3 shows the correlation between the drift of the Sr isotope, defined as $\Delta\varepsilon_{Sr} = \varepsilon_{Sr(SP)} - \varepsilon_{Sr(PR)}$, where SP indicates saprolite, PR indicates parent rock. A significant positive correlation is observed between the $\Delta\varepsilon_{Sr}$ and Sr concentrations, with a correlation coefficient of 0.57 ($N = 18$, $p < 0.007$). In particular, in the upper profile where a significant upward increasing trend of ε_{Sr} (samples HK06-1 to HK06-4) exhibits, the correlation coefficient between $\Delta\varepsilon_{Sr}$ and Sr concentrations is up to 0.91 (Fig. 3). Thus, the saprolites in the top profile have higher Sr concentrations and larger ε_{Sr} gaps away from parent rocks. This agrees well with the scenario that extraneous Sr with different Sr isotopic compositions were imported from the top of the saprolite profile, and they were downward transported and consequently trapped by clay minerals in the profile and mixed with the residual Sr in the saprolites.

Extraneous Sr input has generally been observed in soils and saprolite profiles (Price et al., 1991; Stewart et al., 2001; Kurtz et al., 2001; Dia et al., 2006). Possible sources for the extraneous Sr may be meteoric precipitation (both wet and dry deposits), Sr-laden surface runoff, or groundwater. There is no permanent surface runoff around the profile, and the landform of this profile is a hill, which locates several meters above the drainage for surface runoff formed by rainwater. Moreover, the upper profile is well above the average groundwater level in this region (Ma et al., 2007a). Thus, surface runoff and groundwater appear not to contribute much extraneous Sr to the saprolites at the upper profile. Meanwhile, the $^{87}Sr/^{86}Sr$ of the topmost sample in our profile is 0.709370 ± 7, which is similar to that in modern seawater, about 0.7092. Considering that the distance from the location of our profile to the South China Sea is less than 20 km, seawater may be the possible source for the extraneous Sr input to our profile. This can be inferred from the fairly high Sr and Na concentrations of the precipitation in Sanya (Table 2). Sr concentrations in rainwater

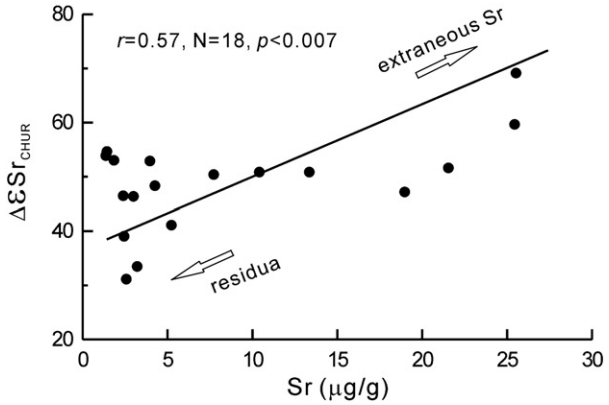

Fig. 3. Correlation between Sr concentrations and ε_{Sr} drifts ($\Delta\varepsilon_{Sr}$) of the saprolites from the parent rock.

precipitated during summer are up to 139 μg/L. The about 1500 mm annual precipitation amount in this region continuously imports the extraneous Sr to the profile, and the consecutively trapping of Sr by clay minerals may accumulate enough Sr to the concentration of the top saprolites, about 25 μg/g. Moreover, the Sr in the precipitation is closely associated with Na, with correlation coefficient between Sr and Na concentrations of about 0.87 ($N=4$). As Na is characteristically from seawater, such correlation, as well as the close to seawater $^{87}Sr/^{86}Sr$ ratio of the top saprolite, suggests that the extraneous Sr mainly from seawater may significantly influence the Sr isotopes of the saprolites of the upper profile.

4.1.2. Variations of the Nd and Hf isotopes

Nd is a moderate mobile element during chemical weathering. It can be easily motivated from primary minerals and tends to be fixed in weathering products during incipient-to-moderate weathering. However, it can be removed during intensive weathering (Nesbitt et al., 1980; Nesbitt and Wilson, 1992). The distribution of Nd in this profile exhibits such behavior well. As shown in Fig. 4a, significant loss of Nd is observed in the top section, above 3.0 m, with a lower Nd/Th ratio compared to the parent rock's. Correspondingly, significant Nd enrichment occurs in the lower section, with a raised Nd/Th of up to 387%; i.e., about 4 times the enrichment for Nd. The storage of the enriched REEs in this profile is complicated. Elemental analysis on the bulk saprolites indicates that Mn oxides/hydroxides, as well as secondary phosphate minerals and Fe oxides/hydroxides are possible hosts for the REEs in this profile (Ma et al., 2007a). Further HCl-acid leaching tests on these saprolites indicate that over 80% of the REEs can be leached by diluted HCl acid, and the extractable REEs are closely associated with extractable Al and Mn, suggesting that these REEs are loosely combined with clay minerals (Ma et al., 2007b). This can also be inferred from the distribution of water-bearing clay minerals (halloysite + gibbsite) in this profile (Fig. 4). The abundance of halloysite + gibbsite shows similar variation trend with the percentage change of Nd/Th ratio, and moderate positive correlation with coefficient of 0.61 ($N=15$, $p<0.008$) is observed between them. Accompanying such re-distribution of Nd, the $^{143}Nd/^{144}Nd$ ratios are significantly lower in the saprolites than in the parent rock (Table 1). The ε_{Nd} drifts, expressed as $\Delta\varepsilon_{Nd}$, representing the difference between the saprolites and the parent rock, are all negative, from −0.15 to −2.58. In particular, the ε_{Nd} drifts are generally more negative in the top section, where chemical weathering was more intensive, than those in the lower section. A moderate positive correlation is observed between the ε_{Nd} drifts and the percentage changes of Nd/Th ratios in the saprolites, with a correlation coefficient of about 0.51 ($N=18$, $p<0.015$). This indicates that the larger proportionate loss of Nd may result in more negative drift of $^{143}Nd/^{144}Nd$ in the saprolites, relative to the parent rock.

It is worth noting that in the lower section (<3.0 m), where Nd is significantly enriched, the $\Delta\varepsilon_{Nd}$ values are all negative, though higher than those in the upper section. The enriched Nd in the lower section may generally be comprised of both the Nd removed and transported from the upper section and of that from the sections that have been eroded from the profile (Ma et al., 2007a). The overall negative drift of the ε_{Nd} in the saprolites, compared to that in the parent rock, suggests a net loss of Nd in the whole profile. The removed Nd may have higher $^{143}Nd/^{144}Nd$ ratios, and thus the Nd retained in the saprolites shows more negative ε_{Nd} compared to that of the parent rock. This again agrees with the observations about the upper section.

Hf is believed to be conservative during chemical weathering of basalt (Nesbitt et al., 1980; Nesbitt and Wilson, 1992). However, significant loss of Hf can also be seen during extreme weathering in our profile (Ma et al., 2007a). The percentage changes of the Hf/Th ratios relative to parent rock indicate up to 30% of Hf was lost in the upper section (>3.0 m). The behavior of Hf is very similar to that of Fe in this profile, with correlation coefficient between Hf and Fe concentrations of 0.96 ($N=19$, $p<0.0000001$) (Ma et al., 2007a). Thus, the storage of Hf in the saprolites may be associated with Fe-bearing minerals. Among the detectable Fe-bearing minerals in this profile, ilmenite and magnetite may be the original minerals of the parent rock, and goethite is a typically secondary minerals transformed from original Fe-bearing minerals. Goethite abundance is relatively high in the upper profile, accompanying with Hf loess during intensive chemical weathering. There exhibits a moderate negative correlation between the percentage changes of Hf/Th and goethite abundance with correlation coefficient between of −0.70 ($N=11$, $p<0.008$) (Fig. 4). This appears to indicate that the loss of Hf in the profile is associated with modification of Fe-bearing minerals during intensive weathering. Meanwhile, the loss of Hf is closely related to drifts of Hf isotopes in the profile like that for Nd isotopes. A

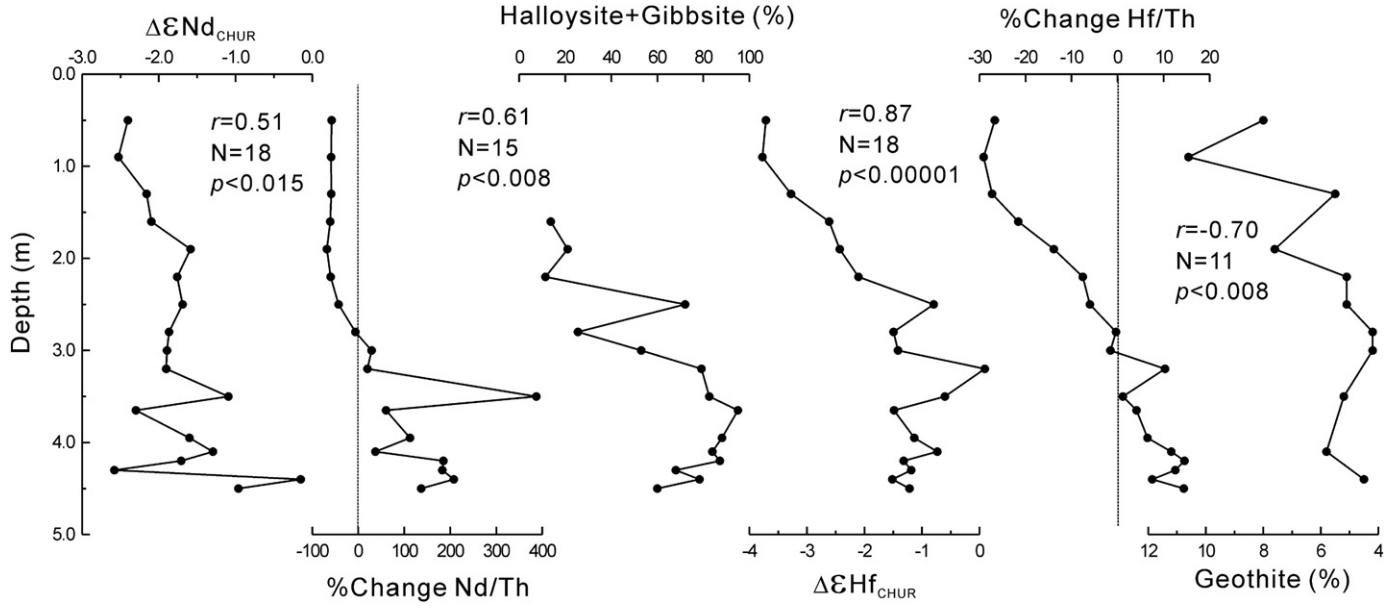

Fig. 4. In-depth variations of the ε_{Nd} and ε_{Hf} drifts ($\Delta\varepsilon_{Nd}$ and $\Delta\varepsilon_{Hf}$) of the saprolites from the parent rock, the percentage changes of the Nd/Th, Hf/Th ratios relative to the parent rock, and the abundance of water-bearing clay minerals (halloysite + gibbsite) and goethite.

significant negative drift of ε_{Hf} occurs in the profile, with $\Delta\varepsilon_{Hf}$ up to −4.0 (Fig. 4). Significant positive correlation occurs between the $\Delta\varepsilon_{Hf}$ and the percentage changes of Hf/Th, with a coefficient of about 0.87 ($N=18$, $p<0.00001$). Therefore, the loss of Hf induced by extreme chemical weathering appears to preferentially remove ^{176}Hf, and thus the Hf retained in the saprolites may have smaller ε_{Hf} values compared to that of the parent rock.

Similarly, slight enrichment of Hf occurs in the lower section, with percentage changes of Hf/Th of about 0–15% (Fig. 4). The $\Delta\varepsilon_{Hf}$ values increase, but are still negative. As in the case of Nd isotopes, this may be attributed to the net loss of Hf in the profile, compared to the parent rock.

As mentioned above, the import of extraneous materials is the key to control the drift of ε_{Sr} in the upper profile. The input of extraneous Nd and Hf, if there is any, may also result in ε_{Nd} and ε_{Hf} drifts in the upper profile. Similarly, the landform and the groundwater level of this profile as mentioned above suggest that surface runoff and groundwater may not contribute much extraneous Nd and Hf to the profile. On the other hand, wet meteoric precipitation or rainwater has very low Nd and Hf concentrations, under the detection limit of the ICP-MS (<0.01 μg/L) (Table 2). It is not likely for the rainwater to import enough extraneous Nd and Hf that can significantly influence the Nd and Hf isotopic compositions of the saprolites at the upper profile, for the Nd and Hf concentrations in these saprolites are relatively high, at the level of ~25 μg/g and ~13 μg/g, respectively. As for dry meteoric precipitation, dust from the Loess Plateau in North China is one of the most important sources for aeolian precipitation in South China as southward transport of such materials are very prominent during winters by winter monsoon. The loess across the whole Loess Plateau from Jixian at the east to Xining at the west show limited variation range for Nd and Hf concentration and Nd isotopic compositions (Jahn et al., 2001). In details, the Nd concentration in loess generally ranges from 20 μg/g to 30 μg/g (Jahn et al., 2001), which is similar to that in the saprolites at the top section of our profile. The $^{143}Nd/^{144}Nd$ values of the loess generally range from 0.512016 to 0.512147 (Jahn et al., 2001), which are significantly lower than those of the saprolites in our profile. If the significant ε_{Nd} drifts in the upper profile were caused by import of aeolian precipitation, 10–15% of aeolian precipitation import is needed in calculating the two end-member mixing model. Hf isotopic compositions of the loess are not available currently. Considering that the Hf concentration in loess (3–7 μg/g) (Jahn et al., 2001) is significantly lower than those in the upper saprolites of our profile, and the ε_{Hf} drifts in the upper profile are even larger than the ε_{Nd} drifts. A much larger proportion import of aeolian precipitation is needed to drive such ε_{Hf} drifts. Meanwhile, the concentrations of some of the conservative elements, such Ti, Zr, Hf, Nb, Ta and Th, also have limited variation ranges, which are significantly different from those in the saprolites of our profile. Fig. 5 shows the TiO_2*1000/Zr~Th/Nb and Zr/Hf~Nb/Ta diagram of both the loess and saprolites. The gaps between the loess and the saprolites are very large in these diagrams, and there is no sign to support up to 10–15% of even higher import of loess into the saprolites. Therefore, extraneous Nd and Hf imported by dry meteoric precipitation may not be the factor to control the ε_{Nd} and ε_{Hf} drifts in the upper profile. More importantly, if there is some extraneous Nd and Hf imported from the top of the profile, the Nd and Hf concentrations may exhibit an upward increasing trend at the upper profile like that of the Sr concentrations. Both Nd and Hf, however, exhibit enhanced loss in the upper profile (Fig. 4). Thus, the negative ε_{Nd} and ε_{Hf} drifts in the upper profile may not be caused by import of extraneous Nd and Hf, but are resulted by consecutive loss of Nd and Hf during intensive chemical weathering.

Consecutive loss of some elements by incongruent decomposition of minerals during weathering process may result in change in some isotopic composition in saprolites if the isotopic compositions are heterogeneous in different minerals due to long-term uneven accumulation of radiogenic decay. This has been adopted to interpret

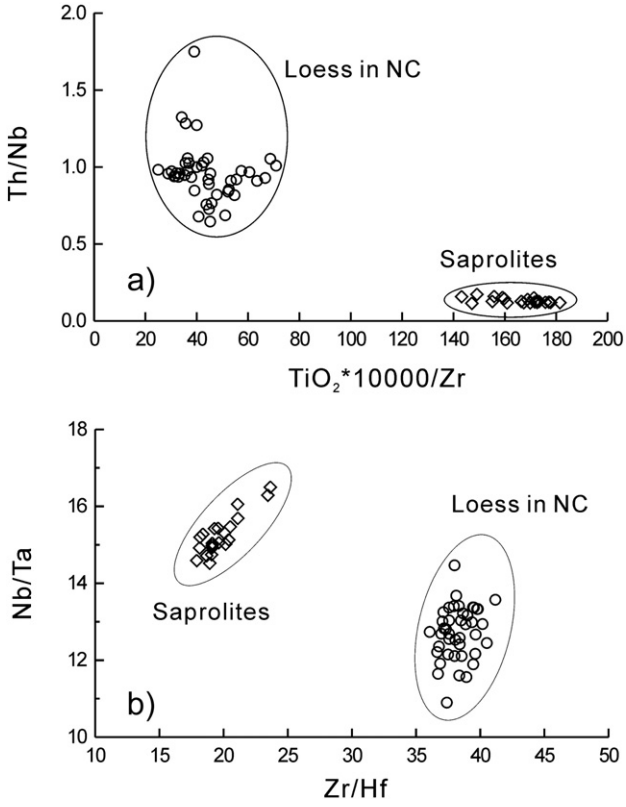

Fig. 5. Diagrams of conservative elements both for the loess from the Loess Plateau in North China and the saprolites in this profile. a) $TiO_2*10{,}000/Zr$~Th/Nb; b) Zr/Hf~Nb/Ta. Data of the loess are from Jahn et al. (2001).

the $^{87}Sr/^{86}Sr$ change in saprolites from incipient basaltic weathering profiles (Nesbitt and Wilson, 1992). However, this seems not to be the case for the Nd and Hf isotope changes in our profile. Assuming that the initial Nd and Hf isotopic compositions of the basalts are homogeneous at its eruption, the initial $^{143}Nd/^{144}Nd$ and $^{176}Hf/^{177}Hf$ ratios of the basalts at ~4.0 Ma are 0.512783 and 0.283039, respectively, calculated from the data in Table 1. Thus, all the minerals in the basalts have $^{143}Nd/^{144}Nd$ and $^{176}Hf/^{177}Hf$ ratios not lower than these values when they start to be decomposed by chemical weathering. It is worth noting that all the $^{143}Nd/^{144}Nd$ and $^{176}Hf/^{177}Hf$ ratios of the saprolites are generally much lower than these values. Simply removal of part of the Nd and Hf by incongruent decomposition of minerals without isotopic fractionation may not result in significant decrease of $^{143}Nd/^{144}Nd$ and $^{176}Hf/^{177}Hf$ ratios in the residues because all the original compositions have high $^{143}Nd/^{144}Nd$ and $^{176}Hf/^{177}Hf$ ratios. Moreover, the weathering intensity in our profile is extremely high, given that nearly all the primary minerals have been altered (Ma et al., 2007a). Thus, most of the Nd and Hf have been activated and re-distributed in secondary minerals. This appears to indicate that fractionation has likely happened during the processes in which Nd and Hf were incorporated into the secondary minerals, such as ion exchange, absorption, or a combination of these. The higher mass isotopes, such as ^{144}Nd and ^{177}Hf, may preferentially be incorporated into the secondary minerals relative to the lower mass isotopes, such as ^{143}Nd and ^{176}Hf. As a result, the $^{143}Nd/^{144}Nd$ and $^{176}Hf/^{177}Hf$ in the saprolites are lower than those in the parent rock. Details of this process are not well known yet. Considering that all the $^{143}Nd/^{144}Nd$ and $^{176}Hf/^{177}Hf$ ratios of the saprolites have been normalized using internal ratios, such as $^{146}Nd/^{144}Nd=0.7219$ and $^{179}Hf/^{177}Hf=0.7325$ for Nd and Hf, respectively during mass spectrometry measurements, if the isotopic fractionation during this process resembles the mass-dependent fractionation, it can be partially compensated. However, the significant Nd and Hf

isotope drifts observed in our profile suggest that such compensate is limited. Thus, more studies, including directly measuring the Nd and Hf isotopes of the removed components during chemical weathering are needed to learn more about this process. Despite of lack of such knowledge currently, our observations clearly show isotope fractionations during extreme chemical weathering processes, even for the isotopic systematics with high masses, such as Nd and Hf.

4.2. Correlations between Nd and Hf isotopes

Similar to the broad positive correlation between $^{143}Nd/^{144}Nd$ and $^{176}Hf/^{177}Hf$ of the global Nd–Hf systems, the Nd and Hf isotopes of the saprolites and parent rock in our profile also exhibit a positive correlation, with a correlation coefficient of about 0.54 ($N=18$, $p<0.01$) as shown in Fig. 5. The paired Hf–Nd isotopic data of some selected modern sediments and basalts (Vervoort et al., 1999; Marini et al., 2005; Van De Flierdt et al., 2007), and of ferromanganese crusts and nodules (Albarede et al., 1998; David et al., 2001), are included to show the terrestrial array and the seawater array, respectively, for comparison. All of our data are located within the range of the terrestrial array, and the negative drift of these Hf and Nd isotopes roughly parallel that of the terrestrial array.

Former studies suggest that inputs of continental Hf released during chemical weathering on continents are the most important factor to control the obliquity of the seawater array away from the terrestrial array (Van De Flierdt et al., 2002, 2004, 2007). The $^{143}Nd/^{144}Nd$ and $^{176}Hf/^{177}Hf$ ratios of the saprolites in our profile are all less than those of the parent rocks, indicating that the released components have higher $^{143}Nd/^{144}Nd$ and $^{176}Hf/^{177}Hf$ ratios than the saprolites. This appears to indicate that the ε_{Nd}–ε_{Hf} correlation of the released components be different from that of the residues during chemical weathering. We can now test the hypothesis in our profile. As shown in the insert at the right corner of Fig. 6, these saprolites are separated into two groups in this diagram. The first group is comprised of the saprolites of the upper 3.0 m, in which the percentage changes of Nd/Th and Hf/Th ratios are negative. Thus, the Nd and Hf in these samples are mainly residual components in saprolites. These Nd and Hf are likely to be trapped more tightly, and tend to be concentrated in sediments when the saprolites are eroded and transported to the ocean. The Nd and Hf isotopes of these samples, together with those of the parent rock, show significant positive correlation, with a correlation coefficient of about 0.83 ($N=10$, $p<0.001$). More importantly, the regression line of these data is parallel to that of the terrestrial array, with a slope of ~1.5 (Fig. 6). This suggests that the variation of the Nd and Hf isotopes trapped in the solid weathering products generally follows that of the terrestrial array. The second group is composed of the saprolites below 3.0 m in this profile. The percentage changes of Nd/Th and Hf/Th ratios of these samples are all positive, indicating Nd and Hf gains. The extra Nd and Hf may mainly be comprised of Nd and Hf released from the upper section of the profile. This can be taken as an analog of continental input into seawater. The ε_{Hf} of these samples are generally higher than those in group one, at a given ε_{Nd}, and their variation trend is close to that of the seawater array (Fig. 6). This provides first-hand evidence, indicating that the $^{176}Hf/^{177}Hf$ and $^{143}Nd/^{144}Nd$ correlation of the Hf and Nd contributed to seawater from chemical weathering release is similar to that of the seawater array. However, these are not the data directly measured on the released components. Moreover, how the Nd and Hf isotopic composition changes during the process for them to be eroded, transported and finally added into the seawater as dissolved components are not known. A lot more studies are needed to answer these questions. Our observation, however, provides hints that the Nd and Hf isotopic composition changes during chemical weathering on continents may significantly contribute to the obliquity of the seawater array away from the terrestrial array of the global Nd and Hf isotope correlation.

4.3. Implications for Sr, Nd, and Hf isotopes as sediment provenance proxies

Sr and Nd isotopes have generally been used to trace provenances of sediments. Considering that sediments are mainly composed of weathering products, the large offsets of the Sr and Nd isotopes between weathering products and parent rocks observed in our profile suggest that the influence of chemical weathering on Sr and Nd isotopes should be carefully considered before using Sr and Nd isotopes as sediment provenance proxies.

The variation range for $^{87}Sr/^{86}Sr$ of the modern weathering products is very large (Goldstein and Jacobson, 1988). Weathering products from basic rocks generally have very low $^{87}Sr/^{86}Sr$, as low as 0.704 ($\varepsilon_{Sr}=-7$), while $^{87}Sr/^{86}Sr$ of weathering products from old crust or alkali granites can be higher than 0.800 ($\varepsilon_{Sr}=1356$) (Goldstein and Jacobson, 1988; Singh et al., 2008). Moreover, the $^{87}Sr/^{86}Sr$ of suspended sediments in large rivers mostly range from 0.71 to 0.73, with ε_{Sr} from about 80 to 360 (Goldstein and Jacobson, 1988). Compared to such a large variation range for Sr isotopes, the ε_{Sr} drift of up to ~70 during extreme chemical weathering observed in our profile seems not to be a serious problem when using Sr isotopes to distinguish basic rock provenances from average continental sources (Asahara et al., 1999; Hemming et al., 2007). However, our results indicate that nearly all the original Sr has been removed and the current Sr is mainly from extraneous sources in the saprolites after intensive weathering. If the Sr isotopic composition was much different from that of the parent rock, the ε_{Sr} drift would be as larger as the gap between basic rocks and average continental sources. Thus, the Sr isotopes of the saprolites do not keep the information their parent rocks, and Sr isotope is not a good fingerprint to trace provenances for sediments and soils undergone intensive chemical weathering.

Compared with Sr isotopes, Nd isotopes are more broadly used in tracing sediment provenances. The variation range of the ε_{Nd} of global sediments is from about −40 to +10 (Goldstein and Jacobson, 1988; Vervoort et al., 1999), which is much larger than the ~2.5 drift of ε_{Nd} during extreme weathering, as observed in our profile. Therefore, the Nd isotope appears to be a good proxy for sediment provenance when the ε_{Nd} variation is not very small (Li et al., 2003; Roy et al., 2007; Gingele et al., 2007).

Hf isotopes are seldom used in tracing sediment provenances because Hf isotopic measurements of sediments are not as broadly available as those for Nd and Sr isotopes. The ε_{Hf} of global sediments vary from about −46 to +8 (Vervoort et al., 1999), which is much larger than the ~3.7 drift of ε_{Hf} during extreme chemical weathering in our profile. Moreover, the ε_{Hf} and ε_{Nd} are highly correlated in sediments, as shown in the terrestrial array (Vervoort et al., 1999). This suggests that the Hf isotope is a potential proxy for sediment provenances such as the Nd isotope. However, when using Nd and Hf isotopes to trace sediment provenances, the drift of ε_{Hf} and ε_{Nd} from extreme chemical weathering, with maxima of −3.7 and −2.5, respectively, should be carefully considered.

5. Summary

The Sr–Nd–Hf isotopic compositions of both the saprolites and parent rocks of an extreme weathering profile developed from Neogene basalts in Hainan, South China are reported in this paper (Fig. 6). All these isotopes show obvious changes in the saprolites compared to those in the parent rocks. $^{87}Sr/^{86}Sr$ shows the maximum variation range, with chondrite-normalized ε_{Sr} of the saprolites drifting away from the parent rock of 30 to 70. The ε_{Nd} and ε_{Hf} drifts of the saprolites away from the parent rocks vary from 0 to −2.6 and from 0 to −3.7, respectively. This indicates significant alteration of these isotopic systematics during extreme chemical weathering. The accumulation of radiogenic ^{87}Sr, ^{143}Nd, and ^{176}Hf may not contribute to such large change of these isotopic systematics given the very young age of the saprolites (<4.0 Ma).

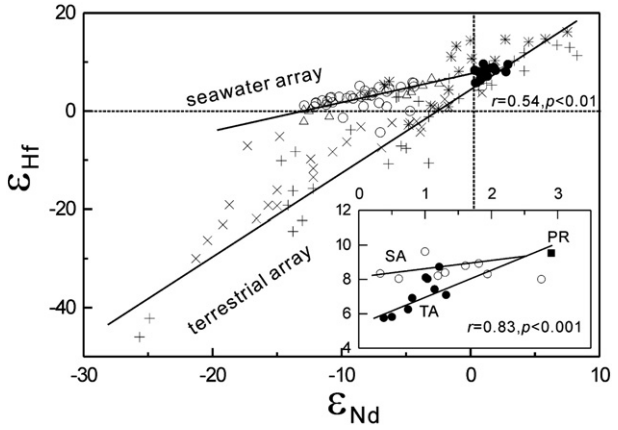

Fig. 6. Correlation between the ε_{Nd} and ε_{Hf} of the saprolites and parent rock. Some selected data are shown in the large diagram to highlight the two arrays, with open circles indicating the ferromanganese crusts and nodules (Albarede et al., 1998; David et al., 2001). Asterisks (*) indicate basalts from Luzon, East of the SCS (Marini et al., 2005), crosses (×) indicate global modern sediments (Vervoort et al., 1999), crosses (+) indicate modern sediments around the Antarctic (van de Flierdt et al., 2007), and solid circles indicate our saprolites. In the inserted diagram, PR, SA, and TA indicate parent rock, seawater arrays, and terrestrial arrays, respectively. Solid circles indicate the saprolites with negative percentage changes of Nd/Th and Hf/Th ratios relative to the parent rock, and open circles indicate those with positive percentage change values.

The main points to be made about such isotopic systematic variations are as follows:

1) Nearly all the Sr in parent rock has been removed from the profile. The ε_{Sr} drift in the saprolites shows an upward increasing trend, co-incident with the increasing Sr concentrations. This suggests that the Sr in the saprolites is mainly imported from extraneous sources, and the Sr isotopic compositions in the saprolites may not represent those of the parent rock.
2) The import of extraneous Nd and Hf to this profile appears negligible, and the Nd and Hf isotope changes in the profile are mainly resulted from preferential removal of these isotopes. The ε_{Nd} and ε_{Hf} of the saprolites are all smaller than the initial values of the parent rock. The negative drifts of the ε_{Nd} and ε_{Hf} are co-incident with the losses of Nd and Hf in the saprolites, with larger Nd and Hf loss proportions corresponding to more negative ε_{Nd} and ε_{Hf} drift. This suggests that ^{143}Nd and ^{176}Hf may be preferentially removed from the profile relative to ^{144}Nd and ^{177}Hf during extreme chemical weathering.
3) Positive correlation is observed between the ε_{Nd} and ε_{Hf} of the saprolites. Particularly, the saprolites with net loss of Nd and Hf show excellent positive correlation, and the regression line parallels to the terrestrial array. The other saprolites with net gain of Nd and Hf generally show higher ε_{Hf} values at giving ε_{Nd} value, and the regression line between these ε_{Nd} and ε_{Hf} appears to parallel to the seawater array. This supports the hypothesis that the contribution of continental Hf from chemical weathering release is the key for the obliquity of the seawater array away from the terrestrial array of the global ε_{Nd} and ε_{Hf} correlation.
4) Such large drifts of ε_{Sr}, ε_{Nd} and ε_{Hf} in saprolites suggest that Sr isotope is not adequate to trace provenances for sediments and soils undergone intensive chemical weathering, and Nd and Hf isotopes are potential provenance indicators but the variation range of these isotopic compositions should be carefully considered when using them to trace provenances for sediments and soils.

Acknowledgements

The authors are most grateful to X. R. Liang of the GIG-CAS for his assistance with the Nd isotopic analysis, and to Q. L. Li and Y. H. Yang of the IGG-CAS for their help with the Sr–Hf isotopic analysis. Discussions with W. D. Sun of the GIG-CAS helped to improve the manuscript. We are grateful for the constructive comments and suggestions of the two anonymous reviewers and Prof. Bourdon, which help to improve the manuscript. This study was supported by the Knowledge Innovation Project of the Chinese Academy of Sciences Grants (KZCX2-YW-138 and KZCX3-SW-152-2), the special project of the GIG-CAS (Grant GIG-07-04), and the National Science Foundation of China Grant (40473012). This is contribution No. IS-1132 from GIG-CAS.

References

Albarede, F., Simonetti, A., Vervoort, J.D., Blichert-Toft, J., Abouchami, W., 1998. A Hf–Nd isotopic correlation in ferromanganese nodules. Geophysical Research Letters 25 (20), 3895–3898.
Asahara, Y., Tanaka, T., Kamioka, H., Nishimura, A., Yamazaki, T., 1999. Provenance of the north Pacific sediments and process of source material transport as derived from Rb–Sr isotopic systematics. Chemical Geology 158 (3–4), 271–291.
Aubert, D., Stille, P., Probst, A., 2001. REE fractionation during granite weathering and removal by waters and suspended loads: Sr and Nd isotopic evidence. Geochimica et Cosmochimica Acta 65 (3), 387–406.
Banfield, J.F., Eggleton, R.A., 1989. Apatite replacement and rare earth mobilization, fractionation, and fixation during weathering. Clays and Clay Minerals 37 (2), 113–127.
Blum, J.D., Erel, Y., 1995. A silicate weathering mechanism linking increases in marine Sr-87/Sr-86 with global glaciation. Nature 373 (6513), 415–418.
Boulange, B., Colin, F., 1994. Rare-earth element mobility during conversion of nepheline syenite into lateritic bauxite at Passa-Quatro, Minais-Gerais, Brazil. Applied Geochemistry 9 (6), 701–711.
Braun, J.J., Pagel, M., Herbillon, A., Rosin, C., 1993. Mobilization and redistribution of REEs and thorium in a syenitic lateritic profile — a mass-balance study. Geochimica et Cosmochimica Acta 57 (18), 4419–4434.
Braun, J.J., Viers, J., Dupre, B., Polve, M., Ndam, J., Muller, J.P., 1998. Solid/liquid REE fractionation in the lateritic system of Goyoum, east Cameroon: the implication for the present dynamics of the soil covers of the humid tropical regions. Geochimica et Cosmochimica Acta 62 (2), 273–299.
Chesworth, W., Dejou, J., Larroque, P., 1981. The weathering of basalt and relative mobilities of the major elements at Belbex, France. Geochimica et Cosmochimica Acta 45, 1235–1243.
Condie, K.C., Dengate, J., Cullers, R.L., 1995. Behavior of rare-earth elements in a paleoweathering profile on granodiorite in the Front Range, Colorado, USA. Geochimica et Cosmochimica Acta 59 (2), 279–294.
David, K., Frank, M., O'Nions, R.K., Belshaw, N.S., Arden, J.W., 2001. The Hf isotope composition of global seawater and the evolution of Hf isotopes in the deep Pacific Ocean from Fe–Mn crusts. Chemical Geology 178 (1–4), 23–42.
De Souza, G.F., Reynolds, B.C., Bourdon, B., 2007. Evidence for stable strontium isotope fractionation during chemical weathering. Geochimica et Cosmochimica Acta 71 (15), A220.
Dia, A., Chauvel, C., Bulourde, M., Gerard, M., 2006. Eolian contribution to soils on Mount Cameroon: isotopic and trace element records. Chemical Geology 226 (3–4), 232–252.
Duddy, L.R., 1980. Redistribution and fractionation of rare-earth and other elements in a weathering profile. Chemical Geology 30, 363–381.
Faure, G., Mensing, T.M., 2005. Isotopes: Principles and Applications. Wiley, Hoboken, N.J.
Gingele, F., De Deckker, P., Norman, M., 2007. Late Pleistocene and Holocene climate of SE Australia reconstructed from dust and river loads deposited offshore the River Murray Mouth. Earth and Planetary Science Letters 255 (3–4), 257–272.
Goldstein, S.L., Jacobson, S.B., 1988. Nd and Sr isotopic systematics of river water suspended material: implications for crustal evolution. Earth and Planetary Science Letters 87, 249–265.
Hemming, S.R., van de Flierdt, T., Goldstein, S.L., Franzese, A.M., Roy, M., Gastineau, G., Landrot, G., 2007. Strontium isotope tracing of terrigenous sediment dispersal in the Antarctic Circumpolar Current: implications for constraining frontal positions. Geochemistry Geophysics Geosystems 8, Q06N13. doi:10.1029/2006GC001441.
Hill, I.G., Worden, R.H., Meighan, I.G., 2000. Yttrium: the immobility–mobility transition during basaltic weathering. Geology 28 (10), 923–926.
Jahn, B.M., Gallet, S., Han, J.M., 2001. Geochemistry of the Xining, Xifeng and Jixian sections, Loess Plateau of China: eolian dust provenance and paleosol evolution during the last 140 ka. Chemical Geology 178 (1–4), 71–94.
Koppi, A.J., Edis, R., Field, D.J., Geering, H.R., Klessa, D.A., Cockayne, D.J.H., 1996. Rare earth element trends and cerium–uranium–manganese associations in weathered rock from Koongarra, northern territory, Australia. Geochimica et Cosmochimica Acta 60 (10), 1695–1707.
Kurtz, A.C., Derry, L.A., Chadwick, O.A., 2001. Accretion of Asian dust to Hawaiian soils: isotopic, elemental, and mineral mass balances. Geochimica et Cosmochimica Acta 65 (12), 1971–1983.
Li, X.H., Wei, G.J., Shao, L., Liu, Y., Liang, X.R., Han, Z.M., Sun, M., Wang, P.X., 2003. Geochemical and Nd isotopic variations in sediments of the South China Sea: a response to Cenozoic tectonism in SE Asia. Earth and Planetary Science Letters 211 (3–4), 207–220.

Li, X.H., Qi, C.S., Liu, Y., Liang, X.R., Tu, X.L., Xie, L.W., Yang, Y.H., 2005. Rapid separation of Hf from rock samples for isotope analysis by MC-ICPMS: a modified single-column extraction chromatography method (in Chinese with English abstract). Geochimica (Beijing) 34 (2), 109–114.

Liang, X.R., Wei, G.J., Li, X.H., Liu, Y., 2003. Precise measurement of $^{143}Nd/^{144}Nd$ and Sm/Nd ratios using multiple-collectors inductively coupled plasma-mass spectrometry (MC-ICPMS) (in Chinese with English abstract). Geochimica 32 (1), 91–96.

Ma, J.L., Wei, G.J., Xu, Y.G., Long, W.G., Sun, W.D., 2007a. Mobilization and re-distribution of major and trace elements during extreme weathering of basalt in Hainan Island, South China. Geochimica et Cosmochimica Acta 71 (13), 3223–3237.

Ma, J.L., Wei, G.J., Xu, Y.G., 2007b. Relationship between REE and Al, P, Fe and M n in basaltic weathering products: evidences from hydrochloric acid leaching (in Chinese with English abstract). Geochimica (Beijing) 36 (6), 638–644.

Marini, J.C., Chauvel, C., Maury, R.C., 2005. Hf isotope compositions of northern Luzon arc lavas suggest involvement of pelagic sediments in their source. Contributions to Mineralogy and Petrology 149 (2), 216–232.

Marsh, J.S., 1991. REE fractionation and Ce anomalies in weathered Karoo dolerite. Chemical Geology 90 (3–4), 189–194.

Middelburg, J.J., Van der Weijden, C.H., Woittiez, J.R.W., 1988. Chemical processes affecting the mobility of major, minor and trace elements during weathering of granitic rocks. Chemical Geology 68, 253–273.

Mongelli, G., 1993. Ree and other trace-elements in a granitic weathering profile from Serre, Southern Italy. Chemical Geology 103 (1–4), 17–25.

Nahon, D., Paquet, H., Delvigne, J., 1982. Lateritic weathering of ultramafic rocks and the concentration of nickel in the western Ivory-Coast. Economic Geology 77 (5), 1159–1175.

Negrel, P., 2006. Water–granite interaction: clues from strontium, neodymium and rare earth elements in soil and waters. Applied Geochemistry 21 (8), 1432–1454.

Nesbitt, H.W., 1979. Mobility and fractionation of rare earth elements during weathering of granodiorite. Nature 279, 206–210.

Nesbitt, H.W., Markovics, G., 1997. Weathering of granodioritic crust, long-term storage of elements in weathering profiles, and petrogenesis of siliciclastic sediments. Geochimica et Cosmochimica Acta 61 (8), 1653–1670.

Nesbitt, H.W., Wilson, R.E., 1992. Recent chemical-weathering of basalts. American Journal of Science 292 (10), 740–777.

Nesbitt, H.W., Markovics, G., Price, R.C., 1980. Chemical processes affecting alkalis and alkaline earths during continental weathering. Geochimica et Cosmochimica Acta 44, 1659–1666.

Nowell, G.M., Kempton, P.D., Noble, S.R., Fitton, J.G., Saunders, A.D., Mahoney, J.J., Taylor, R.N., 1998. High precision Hf isotope measurements of MORB and OIB by thermal ionisation mass spectrometry: insights into the depleted mantle. Chemical Geology 149, 211–233.

Ohlander, B., Ingri, J., Land, M., Schoberg, H., 2000. Change of Sm–Nd isotope composition during weathering of till. Geochimica et Cosmochimica Acta 64 (5), 813–820.

Patino, L.C., Velbel, M.A., Price, J.R., Wade, J.A., 2003. Trace element mobility during spheroidal weathering of basalts and andesites in Hawaii and Guatemala. Chemical Geology 202 (3–4), 343–364.

Price, R.C., Gray, C.M., Wilson, R.E., Frey, F.A., Taylor, S.R., 1991. The effects of weathering on rare-earth element, Y and Ba abundances in tertiary basalts from southeastern Australia. Chemical Geology 93 (3–4), 245–265.

Roy, M., van de Flierdt, T.V., Hemming, S.R., Goldstein, S.L., 2007. Ar-40/Ar-39 ages of hornblende grains and bulk Sm/Nd isotopes of circum-Antarctic glacio-marine sediments: implications for sediment provenance in the southern ocean. Chemical Geology 244 (3–4), 507–519.

Singh, S.K., Rai, S.K., Krishnaswami, S., 2008. Sr and Nd isotopes in river sediments from the Ganga Basin: sediment provenance and spatial variability in physical erosion. Journal of Geophysical Research-Earth Surface 113 (F3), F03006. doi:10.1029/2007JF000909.

Stewart, B.W., Capo, R.C., Chadwick, O.A., 2001. Effects of rainfall on weathering rate, base cation provenance, and Sr isotope composition of Hawaiian soils. Geochimica et Cosmochimica Acta 65 (7), 1087–1099.

Stirling, C.H., Andersen, M.B., Potter, E.K., Halliday, A.N., 2007. Low-temperature isotopic fractionation of uranium. Earth and Planetary Science Letters 264 (1–2), 208–225.

van de Flierdt, T., Frank, M., Lee, D.C., Halliday, A.N., 2002. Glacial weathering and the hafnium isotope composition of seawater. Earth and Planetary Science Letters 198 (1–2), 167–175.

van De Flierdt, T., Frank, M., Lee, D.C., Halliday, A.N., Reynolds, B.C., Hein, J.R., 2004. New constraints on the sources and behavior of neodymium and hafnium in seawater from Pacific Ocean ferromanganese crusts. Geochimica et Cosmochimica Acta 68 (19), 3827–3843.

van de Flierdt, T., Goldstein, S.L., Hemming, S.R., Roy, M., Frank, M., Halliday, A.N., 2007. Global neodymium–hafnium isotope systematics — revisited. Earth and Planetary Science Letters 259 (3–4), 432–441.

Vervoort, J.D., Patchett, P.J., Blichert-Toft, J., Albarede, F., 1999. Relationships between Lu–Hf and Sm–Nd isotopic systems in the global sedimentary system. Earth and Planetary Science Letters 168 (1–2), 79–99.

Walter, A.V., Nahon, D., Flicoteaux, R., Girard, J.P., Melfi, A., 1995. Behaviour of major and trace elements and fractionation of REE under tropical weathering of a typical apatite-rich carbonatite from Brazil. Earth and Planetary Science Letters 136 (3–4), 591–602.

Wei, G.J., Liu, Y., Tu, X.L., Liang, X.R., Li, X.H., 2004. Separation of Sr, Sm and Nd in mineral and rock samples using selective specific resins (in Chinese with English abstract). Rock and Mineral Analysis 23, 11–14.

Wiederhold, J.G., Teutsch, N., Kraemer, S.M., Halliday, A.N., Kretzschmar, R., 2007. Iron isotope fractionation in oxic soils by mineral weathering and podzolization. Geochimica et Cosmochimica Acta 71 (23), 5821–5833.

Wimpenny, J., Gannoun, A., Burton, K.W., Widdowson, M., James, R.H., Gislason, S.R., 2007. Rhenium and osmium isotope and elemental behaviour accompanying laterite formation in the Deccan region of India. Earth and Planetary Science Letters 261 (1–2), 239–258.

Yamaguchi, K.E., Johnson, C.M., Beard, B.L., Beukes, N.J., Gutzmer, J., Ohmoto, H., 2007. Isotopic evidence for iron mobilization during Paleoproterozoic lateritization of the Hekpoort paleosol profile from Gaborone, Botswana. Earth and Planetary Science Letters 256 (3–4), 577–587.

Zhu, B.Q., Wang, H.F., 1989. Nd–Sr–Pb isotopic and chemical evidence for the volcanism with ORB-OIB source characteristics in the Leiqiong Area, China. Geochimica (Beijing) 18 (3), 193–201.